

Three-phase full-wave diode rectifier with DC voltage stabilization

Abstract. This paper deals with the design and fabrication of a three-phase full-wave diode rectifier, which is based on an industrial modular bridge circuit consisting of six semiconductor diodes. Special attention is given to the design of DC voltage stabilization with film capacitors, which have extremely low series resistances and inductances. Thus, within the framework of this paper, a stabilized rectifier with a nominal power of 270 kW and a maximum current of 300 A was made. Various tests have been conducted to evaluate the rectifier's performance, affirming its practical applicability.

Streszczenie. Artykuł dotyczy zaprojektowania i wykonania trójfazowego pełnokresowego prostownika diodowego, który jest oparty na przemysłowym modułowym obwodzie mostkowym składającym się z sześciu diod półprzewodnikowych. Szczególną uwagę zwrócono na konstrukcję układu stabilizacji napięcia stałego z kondensatorami foliowymi, które mają wyjątkowo niskie rezystancje szeregowe i indukcyjności. W ramach pracy wykonano więc prostownik stabilizowany o mocy znamionowej 270 kW i maksymalnym natężeniu prądu 300 A. Przeprowadzono różne testy w celu oceny wydajności prostownika, potwierdzając jego praktyczną przydatność. (Trójfazowy pełnokresowy prostownik diodowy ze stabilizacją napięcia stałego)

Keywords: Diode rectifier, Converter, Film capacitor, DC link.

Słowa kluczowe: Prostownik diodowy, Konwerter, Kondensator foliowy, Łącze DC.

Introduction

Three-phase power electronic conversion systems play a significant role in a variety of applications, including motor drives and renewable energy systems. Power electronic conversion systems are responsible for conditioning electrical power, which involves the control and conversion of one form of electrical power into another form. This may include the conversion between AC and DC, or adjustments in output magnitude, phase or frequency to meet specific application requirements. For instance, applications that involve battery fed systems, three-phase voltage source inverters (VSI) utilizing pulse width modulation (PWM), or motor drives may require multistage power conversion, where two or more converters are connected in series, parallel, or in cascade fashion. General example of such power conversion system structure is presented in Fig. 1. The converter on the source side may be of various structures such as diode/thyristor/transistor rectifiers, DC-DC converters, or passive filters, while the inverter on the load side is typically a three-phase VSI [1,2].

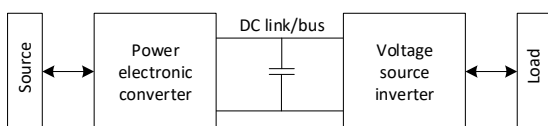


Fig.1. General example of power conversion system structure employing VSI inverter

When an AC-DC conversion stage is used on the source side, input current ripple is injected to the DC link. While diode or thyristor rectifiers create low frequency current ripple, PWM operated transistor rectifiers and inverters produce high frequency current ripple in the DC link. Thus, the DC link capacitor receives harmonic current from both the rectifier and inverter sides, therefore the type and size of the capacitor must be selected accordingly in order to minimize the current and voltage ripple. Typically, electrolytic and film capacitors are used in the DC link. Electrolytic capacitors have a high capacitance to volume ratio, which makes them suitable for reducing DC link ripple,

but they have a considerably high equivalent series resistance (ESR), resulting in a low current rating. The increase in ESR is proportional to the applied voltage, resulting in operational limitations that typically restrict the maximum allowable voltage to below 500V [2]. Film capacitors are a suitable choice for circuits requiring high currents and voltages at the DC link, as they can operate reliably at higher voltage levels.

In this study, a three-phase full-wave diode rectifier has been developed with a rated power of 270 kW, nominal voltage of 900V, and maximum current of 300 A. The DC voltage stabilization design has been given special attention, utilizing film capacitors with low series resistances and inductances, allowing for operation at higher voltage levels than electrolytic capacitors. The rectifier is designed to operate at different supply voltage frequencies and for application employing three-phase voltage source inverter with PWM switching frequencies of 10-20 kHz. As mentioned in [2], the topology of an application dictates the type and size of the appropriate capacitor, since it determines the ripple current frequency spectrum characteristics. Further information regarding DC-link capacitor selection recommendations and design methods for different inverter applications can be found in references [2, 3, 4, 5].

Design and fabrication of a stabilized rectifier

The developed rectifier consists of commercially available components and custom-designed elements. The electrical connections and insulating components have been constructed using specialized software tools, such as Altium Designer and Solidworks, to ensure precise and accurate fabrication. Fig. 2a depicts the schematic diagram of the stabilized rectifier, while Fig. 2b illustrates the physical prototype of the stabilized rectifier. The rectifier design incorporates an industrial modular bridge circuit (1) mounted on a heat sink, comprising of six semiconductor a) No-load test results diodes with integrated temperature sensor. To ensure minimal output voltage ripple, two film capacitors (2) have been connected in parallel to the output terminals of the bridge diode circuit. The film capacitors have been selected for their optimized performance,

featuring low self-inductance when connected to a suitable bus structure, allowing for handling of higher ripple currents with less capacitance, weight, and volume [6]. The specific connection terminal and mounting point requirements of the capacitor demanded a specially designed laminated bus structure (4,5) and insulation layer (3). The laminated bus

structure comprises electrically conductive metal sheets, made of 0.5 mm thick copper Cu-ETP material, separated by a three-layer insulating material. To ensure optimal performance and protection, all components have been enclosed in a robust housing with electrical terminals and adequate ventilation system, as illustrated in Fig. 2b.

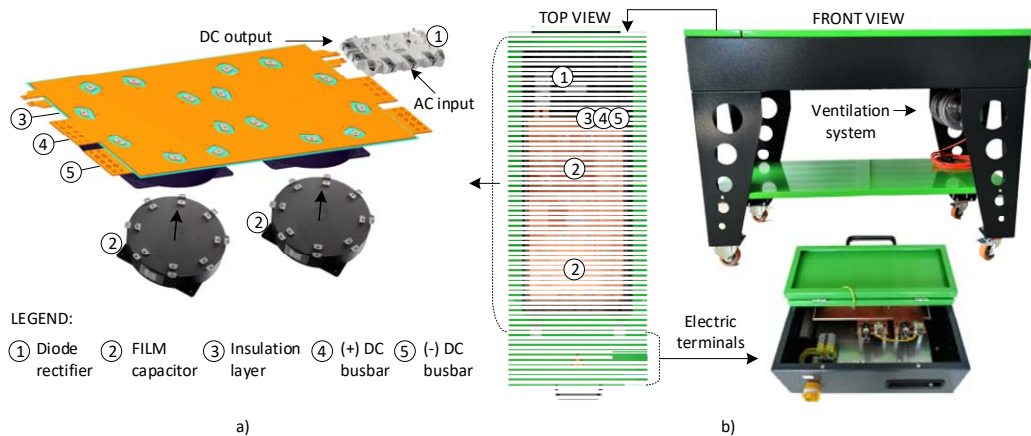


Fig.2. a) Schematic presentation of the stabilized rectifier, b) Stabilized rectifier prototype

Experimental and simulation results

Various tests were conducted on the stabilized rectifier prototype to evaluate its performance, including no-load test, short-circuit test, load test, and temperature rise tests. Hereinafter, all the measured AC electrical quantities are denoted by (\approx), while DC electrical quantities are represented by (=) in the subsequent analysis.

The results of the no-load test at a supply voltage frequency of 50 Hz are presented in Figure 3a and 3b, whereas the results of the short-circuit test are illustrated in Figure 3c. The no-load test, also known as the open-circuit test, is carried out by incrementally raising the input voltage (U_{\approx}) throughout the entire operating range and measuring the output voltage (U_{\approx}) of the stabilized rectifier. The presented time series plot of the output voltage reveals the voltage ripple, which is shown to have a peak to peak value of 0.23 V.

The short-circuit test is carried out by directly short-circuiting the output terminals of the stabilized rectifier and gradually increasing the input voltage (U_{\approx}) in increments, which in turn increases the short-circuit current on the rectifier's DC side until it reaches its nominal value ($I_{(n)}$), as illustrated in Fig. 3c.

In order to evaluate the performance of the stabilized rectifier, a constant inductive resistive load was utilized for both load test and temperature rise test. The load test was conducted at various supply voltage frequencies ranging from 10 Hz to 70 Hz, with a step increment of 10 Hz. During the load test, the load current (I_{\approx}) was gradually increased while simultaneously measuring the AC (P_{\approx}) and DC power ($P_{=}$). By analyzing the results obtained from the load tests, the efficiency of the stabilized rectifier was determined. The load test results are presented in Fig. 4, wherein the power versus load current plot measured at 50 Hz is depicted in Fig. 4a. Furthermore, Fig. 4b illustrates the efficiency surface plot as a function of load current at different supply voltage frequencies.

The power losses (P_{loss}) play a critical role in evaluating the efficiency of the system and determining the necessary cooling requirements. As it can be noticed the efficiency of the stabilized rectifier increases with the load. The comparative analysis of the efficiency of the stabilized rectifier, in relation to a typical rectifier, reveals a relatively low efficiency. This can be attributed to the use of an

inappropriate load during load tests, leading to a relatively high voltage drop across the semiconductor diodes in comparison to the voltage drop across the load. Consequently, the resultant lower efficiency of the system is apparent. However, with an adequate load, the stabilized rectifier is capable of achieving a significantly higher efficiency.

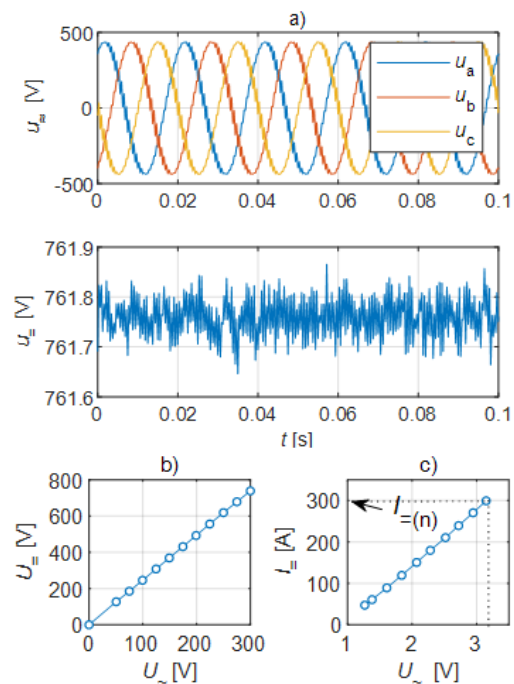


Fig.3. a) Time series plot of a no-load test, b) No-load test results, c) Short-circuit test results

Following the load test the temperature rise test was performed. The temperature rise test results under load conditions ($I_{\approx}=37A$) are shown in Fig. 5, depicting surface temperatures of main components, such as diode, capacitor and heat sink temperatures. The test was performed with the purpose of checking if there are any overheating issues of the components. The temperature rise test is completed after thermal equilibrium is reached and the measured

temperatures begin to stabilize. As it is evident from Fig. 6 there were no overheating problems.

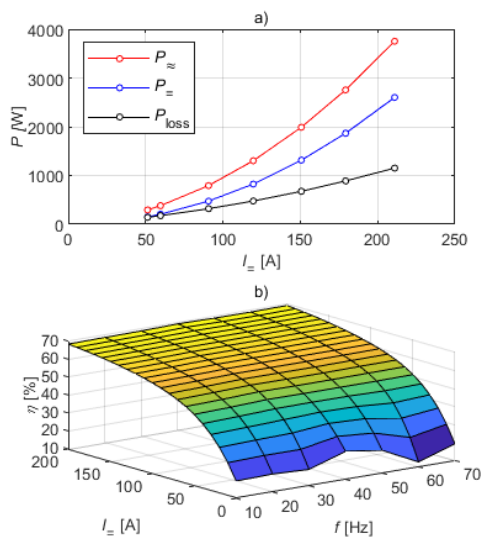


Fig.4. a) Load test results at supply frequency of 50Hz, b) Surface plot of efficiency

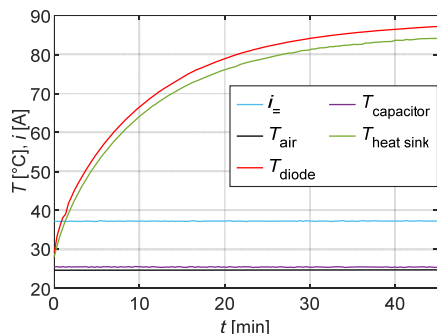


Fig.5. Temperature-rise test results

During the design process, a model of stabilized rectifier (Fig. 6) was also developed using the Matlab Simulink software package. This modelling approach allowed for the creation of a virtual representation of the system, enabling simulation and analysis of its behavior under different operating conditions.

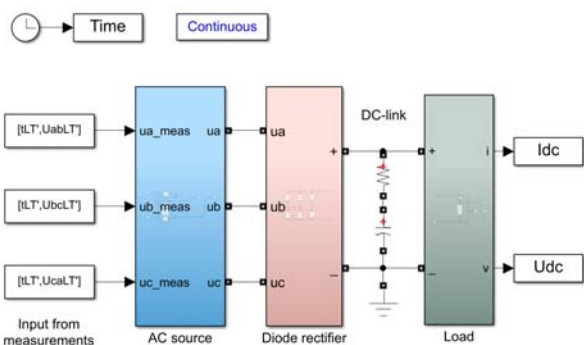


Fig.6. Model of a stabilized rectifier in Matlab Simulink

Fig.7 presents the results of the simulations, along with a comparative analysis of the measurements obtained under load conditions for the stabilized rectifier.

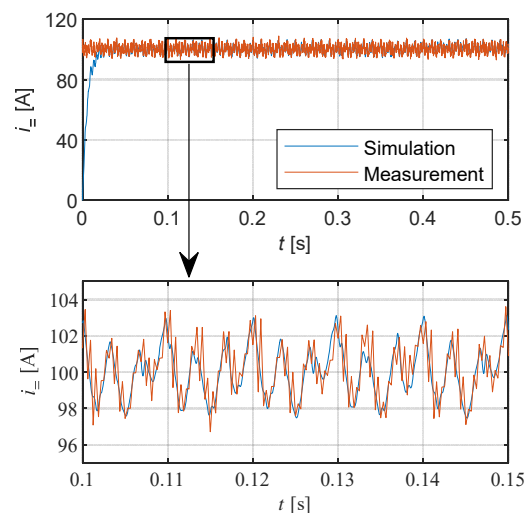


Fig.7. Experimental and simulation results under load conditions

The experimental and simulation results demonstrate a close match, with a visible current ripple present. Specifically, the peak-to-peak value of the current ripple is approximately 6.1 A, which represents a ripple of 5.8% based on the average/DC current value. A stable output under varying load conditions is a critical consideration in practical applications that demand reliable and efficient power conversion. The result of this paper provide valuable insights into the performance of the stabilized rectifier and offer valuable insights for enhancing its design and operation in the future.

Conclusion

This paper covers design and fabrication process of a stabilized rectifier with a nominal power of 270 kW and a maximum current of 300 A. The prototype of stabilized rectifier is also experimentally evaluated by various tests, confirming its applicability in practice. The prototype serves as a good basis for further research work and development. Additional measurement with appropriate load (VSI) are required and a detailed voltage and current spectrum analysis should be done. All measurements were carried out at the Institute of energy technology in the Electric machines and drives laboratory and Applied electrical engineering laboratory.

REFERENCES

- [1] S. Jain, Modeling and Control of Power Electronics Converter System for Power Quality Improvements, *Academic Press*, pp. 31-84, (2018).
- [2] A. M. Hava, U. Ayhan, (2012), "A DC bus capacitor design method for various inverter applications", *IEEE Energy Conversion Congress and Exposition (ECCE)*, pp. 4592-4599.
- [3] R. Grinberg, P.R. Palmer, (2005), "Advanced DC link capacitor technology application for a stiff voltage-source inverter", *IEEE Vehicle Power and Propulsion Conference*, pp. 205-210.
- [4] U. Ayhan, A. M. Hava (2011), "Analysis and characterization of DC Bus ripple current of two-level inverters using the equivalent centered harmonic approach", *IEEE Energy Conversion Congress and Exposition*, pp. 3830-3837.
- [5] A. Safayet, M. Islam, T. Sebastian (2020), "Sizing of DC-link capacitor considering voltage and current ripple requirements", *IEEE Energy Conversion Congress and Exposition*, pp. 1512-1518.
- [6] SBE Power ring film capacitor datasheet: <https://ppmpower.co.uk/wp-content/uploads/SBE-700D590.pdf>.